Analysis of Active Control by Surface Heating

Lucio Maestrello*
California Institute of Technology, Pasadena, California and NASA Langley Research Center, Hampton, Virginia
and
Lu Ting†
New York University, New York, New York

Experiments carried out by Liepmann et al. demonstrate that localized periodic (active) surface heating can excite boundary-layer disturbances, which in turn can be used to cancel or enhance the Tollmien-Schlichting waves. We shall present the theoretical analysis which relates the disturbances in the flowfield to the surface heating. The problem is analyzed by the method of matched asymptotics as a "triple-deck" problem. For water the problem can be linearized. The analysis confirms that small amounts of localized active surface heating can excite local disturbances which increase the momentum near the wall, make the velocity profile fuller, and reduce the displacement thickness. These effects are considered favorable for delaying the onset of instability and separation.

I. Introduction

THE control of laminar-turbulent transition in a boundary layer for drag reduction has been of great importance to airplane design. There are extensive studies of passive control devices, for example: suction or injection, uses of additives, flexible surfaces, trip wires (see, e.g., Ref. 1). Recently Liepmann and his colleagues at the California Institute of Technology pioneered a new active control technique.[2-4] They demonstrated that localized periodic (active) surface heating can be used to excite controlled boundary-layer disturbances either to cancel or to trip the Tollmien-Schlichting (T-S) waves. Experiments were carried out in the water tunnel and in the wind tunnel.

It was demonstrated that small temperature fluctuations (5°C) created by a few narrow strips (of total width 6 to 10 times the displacement thickness) can effectively change the Tollmien-Schlichting wave (for water). This new control technique is very promising since the power requirement is very low and changes in the amplitude, frequency, and phase of the temperature can be made almost instantaneously. In their analysis the thermal sublayer is assumed to be much less than the local boundary layer and is analyzed by the integral method for a steady two-dimensional incompressible flow. A heuristic argument was presented to explain the equivalence between heat flux and an effective normal velocity at the wall, since the coupling between the thermal and mechanical effects is provided by the dependence of viscosity on temperature. Qualitative effects on the stabilization (or destabilization) of the boundary layer due to heating (or cooling) were then obtained for water since the viscosity μ^* decreases as temperature T^* increases, i.e.,

$$\frac{d\mu^*}{dT^*} < 0 \quad \text{for water} \tag{1a}$$

For air the effect of surface temperature control is opposite to that for water since

$$\frac{d\mu^*}{dT^*} > 0 \quad \text{for air} \tag{1b}$$

Here we use (*) to indicate the dimensional quantities.

It is well known that surface suction, which removes the low momentum stream in the inner boundary layer, makes the velocity profile fuller near the wall and results in a thinner displacement thickness. Thus a favorable velocity profile is created, i.e., it is more stable and less prone to separation than the profile without suction.[1]

Surface heating changes the velocity profile due to the dependence of viscosity on temperature. There is an extra term $(d\mu^*/dT^*)(\partial T^*/\partial y^*)(\partial u^*/\partial y^*)$ on the right side of the momentum equation for an incompressible boundary layer where y^* is the coordinate normal to the surface. Since both $(\partial u^*/\partial y^*)$ and $(-\partial T^*/\partial y^*)$ are positive and decrease to zero as y^* increases, and $(d\mu^*/dT^*)$ is negative for water, the extra term represents an increment of momentum. The resulting profile is then fuller near the wall with a thinner displacement thickness, i.e., a more favorable profile. Thus a qualitative argument is presented for the favorable effect of steady surface heating for water and the opposite effect for air due to Eq. (1b).

In the experiments, thin strips are heated by electric current with a frequency ω^*. With the power proportional to $\cos^2\omega^* t$, the temperature of a heating strip T_w^*, can be written as $T_0^* + 2T_I^*\cos^2\omega^* t^*$, where T_0^* is the adiabatic wall temperature. The temperature deviation becomes

$$\Delta T^* = T_w^* - T_0^* = T_I^* + T_I^*\cos 2\omega^* t^* \tag{2}$$

It is composed of a steady term T_I^* and an oscillatory term with amplitude T_I^* and frequency $2\omega^*$. Since the thermal conductivity of the heating strip is much larger than that of water, T_I^* can be considered uniform for each strip but can be different for different strips. By adjusting the amplitudes and the phases of the power inputs to the strips, the induced disturbances in the boundary layer can thereby be controlled to be either in phase or of opposite phase with, i.e., to enhance or annihilate, the T-S waves existing upstream or downstream of the heating strips. For the oscillatory term alone, a change from heating to cooling, i.e., the sign of ΔT^*, or a change in the sign of $d\mu^*/dT^*$ can now be compensated for by a change in phase. It is clear that both the steady and the oscillatory terms can contribute to boundary

Presented as Paper 84-0173 at the AIAA 22nd Aerospace Sciences Meeting, Reno, Nev., Jan. 9-12, 1984; received March 29, 1984; revision received Aug. 24, 1984.

*Visiting Scientist, Graduate Aeronautics Laboratory, 1983-84, on leave from NASA Langley Research Center under Floyd Thompson Fellowship. Associate Fellow AIAA.

†Professor of Mathematics, Courant Institute of Mathematical Sciences. Member AIAA.

controls but they play by different rules. The effects of the steady term depend on the sign of ΔT^* (heating or cooling) and the sign of $d\mu^*/d\tau^*$ (air or water). The effects of the oscillatory term depend on the frequency and the phase relative to T-S waves. The first step for the study of the effects of the steady and the oscillatory terms is to evaluate the disturbances induced by the heating strips, i..e, the changes in velocity profiles and pressure distribution. The favorable effect of the steady solution can then be assessed. The next step will be to study the interaction of the induced disturbances with the T-S waves.

In this paper we shall carry out the first step. We shall use the method of matched asymptotics to relate the temperature, velocity, and pressure disturbances to the local surface heating. The analysis shall include the unsteady effects. Due to the heating elements, the thermal boundary condition is suddenly changed, say, at $x^*=L$ from the adiabatic condition for $x^*<L$ to that of a prescribed temperature for $L<x^*<L+b^*$, where b^* is the total width of the heating elements (see Fig. 1). It is well known that such a sudden change of boundary condition creates a disturbed flowfield in the boundary layer in the neighborhood of $x^*=L$. The local disturbed field can be subdivided into three layers known as the triple deck governed by different sets of approximate equations for each deck and joined to each other by the matching conditions. The necessity of the triple deck, the appropriate scaling and the analyses were formulated independently by Messiter[5] and Stewartson[6] for the flow near the trailing edge of a flat plate. The triple-deck analysis has been applied to many problems in boundary layers with sudden change of wall velocity or external pressure and numerical schemes have been developed for the linear and nonlinear problems.[7-16] Additional references can be found in the two review papers by Stewartson[7] and Smith.[13] The present problem differs from those because we have a sudden change in thermal boundary condition. The analysis has to begin with the energy equation even for an incompressible flow. Since the temperature variations in the water tunnel tests are small, the problem can be linearized. The formulation of the linearized triple-deck problem is outlined in the next section. The solutions for the temperature, velocity, and pressure perturbations are presented in Secs. III and IV. The numerical results and their relevance to boundary-layer control are presented in Sec. V.

II. The Linear Triple Deck

Figure 1 shows the flowfield and the triple-deck structure along a semi-infinite flat plate, the positive x^* axis, near $x^*=L$. The plate is insulated except for the narrow strip $L<x^*<L+b^*$ where the heating elements are placed. For its analysis, the small expansion parameter ϵ is introduced

$$\epsilon = Re^{-1/8} = [U_\infty^*/\nu_\infty^* L]^{-1/8} \tag{3}$$

where Re is the Reynolds number at $x^*=L$ based on the freestream velocity U_∞^* and the kinematic viscosity at the freestream temperature T_∞^*. We note that the displacement thickness of the regular boundary layer at $x^*=L$ is

$$\delta^* = \mathcal{O}(\epsilon^4) \tag{4}$$

The width of the triple deck is of the order of $\epsilon^3 L$. Therefore, the scaled variable for x^* should be

$$x = (x^*-L)/L\epsilon^3 \tag{5}$$

Since the "optimal" total length b^* of the heating elements in the experiments was found to be $6\delta^*$ to $10\delta^*$,[2,3] we can therefore embed the surface heating elements inside the triple deck as shown in Fig. 1 and introduce the nondimensional width b, with $b=b^*/L\epsilon^3$.

The analysis of a triple deck, i.e., the appropriate scaling, the expansion schemes, and the derivation of the governing equations, has been well documented.[7,13] Hence, we shall restate only those which are necessary for the analysis and the assessments of the results and emphasize those which differ from the standard linearized incompressible triple-deck analysis.

The reference scales for the thicknesses of the triple deck are indicated in Fig. 1. The dimensional variable y^* is scaled by $L\epsilon^3$, $L\epsilon^4$, and $L\epsilon^5$ to $\bar{y}$, y, and $\tilde{y}$, respectively. Here we use $(\bar{\ })$ and $(\tilde{\ })$, respectively, to indicate the scaled quantities in the upper and lower deck to differentiate from those in the main deck. The velocity, temperature, and pressure are nondimensionalized by U_∞^*, T_0^*, and $\rho^* U_\infty^{*2}$, respectively. Let $U_B(y)$, $T_B(y)$, and p_∞ denote the scaled horizontal velocity, temperature, and pressure of the boundary layer at $x^*=L$ in absence of the heating strips.

The small temperature variations on the heating strips introduce another small parameter $\alpha = T_R^*/T_0^*$ where T_R^* is a typical value for the temperature deviations, T_I^* in Eq. (2), for the heating strips. We shall consider α and ϵ to be of the same order. Consequently, the perturbation solutions will include both the α-order and the ϵ-order terms and remain valid for $\alpha \gg \epsilon$ and for $\epsilon \ll \alpha$. Since our problem is linear, we shall replace the ratio $\kappa=\alpha/\epsilon$ by unity, construct the solutions, and then insert the appropriate factor $\kappa(T_I^*/T_R^*)$ for each heating strip. In a linearized triple deck,[7,13] an ϵ-order (or α-order) change in the surface temperature induces ϵ^2-order change in $\tilde{u}$ and ϵ^3-order change in $\tilde{v}$ in the lower deck and an ϵ^2-order change in pressure across the triple deck. Of course the ϵ^2-order and ϵ^3-order terms include implicitly the $\epsilon\alpha$-order and $\epsilon^2\alpha$-order terms, respectively.

For the unsteady part, there is another parameter, the Strouhal number $St=\omega^* L/U_\infty^*$. When $St \gg \epsilon^2$ the unsteady term dominates the convection term and the unsteady effect will be confined in a layer much thinner than the lower deck. For $St \ll \epsilon^2$, the unsteady term is of higher order and the leading solution is quasisteady. The governing equations in the lower deck will retain both the unsteady and the convection term when ϵ^2 and St are of the same order.[8,12] Hence, the time variable t will be scaled by $(L/U_\infty^*)\epsilon^2$.

Following the linearized triple-deck analysis, the disturbance pressure in the lower and the main deck can be written as

$$p(s,t) - p_\infty = \epsilon^3 p^{(3)}(x,t) + \mathcal{O}(\epsilon^4) \tag{6}$$

For the lower deck the temperature deviation and velocity components can be written as

$$\bar{T}(x,\bar{y},t,\epsilon) - 1 = \epsilon \bar{T}^{(1)}(x,\bar{y},t) + \mathcal{O}(\epsilon^2) \tag{7a}$$

$$\tilde{u}(x,\tilde{y},t,\epsilon) = \epsilon\beta\tilde{y} + \epsilon^2 \tilde{u}^{(2)}(x,\tilde{y},t) + \mathcal{O}(\epsilon^3) \tag{7b}$$

and

$$\tilde{v}(x,\tilde{y},t,\epsilon) = \epsilon^4 \tilde{v}^{(4)}(x,\tilde{y},t) + \mathcal{O}(\epsilon^5) \tag{7c}$$

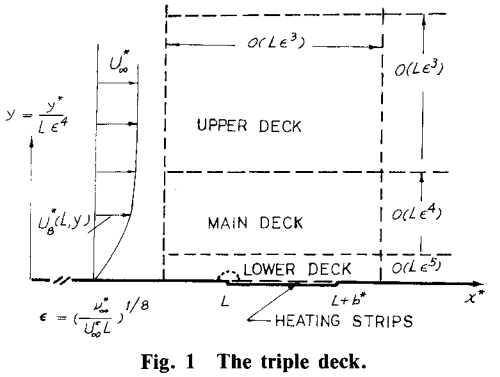

Fig. 1 The triple deck.

where β is the slope of the velocity profile at the wall, i.e., $U_B'(0)$. For the Blasius profile $\beta = 0.33206$.[1] The superscripts in the expansion schemes are identified with the corresponding powers of ϵ, so that it will be easier to recognize the order of the perturbation solutions. The governing equations for the inner deck are

$$\bar{u}_{\bar{x}}^{(2)} + \bar{v}_{\bar{y}}^{(4)} = 0 \tag{8a}$$

$$\bar{u}_{\bar{t}}^{(2)} + \beta\bar{y}\bar{u}_{\bar{x}}^{(2)} + \beta\bar{v}^{(4)} = -p_{\bar{x}}^{(3)}(x,t) + \bar{u}_{\bar{y}\bar{y}}^{(2)} + \Lambda\beta\bar{T}_{\bar{y}}^{(1)} \tag{8b}$$

and

$$\bar{T}_{\bar{t}}^{(1)} + \beta\bar{y}\bar{T}_{\bar{x}}^{(1)} = (Pr)^{-1}\bar{T}_{\bar{y}\bar{y}}^{(1)} \tag{8c}$$

where Λ is equal to $d\ell n\nu^*/d\ell nT^*$ and Pr is the Prandtl number at T_0^*.

In the usual linearized incompressible equations for the inner deck, the unsteady term and the last term in Eq. (8b) are absent and the energy equation for temperature is not needed for the solution of the velocity disturbances. It should be pointed out here that in the boundary-layer solution for $x^* < L$, we have ignored the variation of viscosity with temperature since the maximum variation $(T_0^* - T_\infty^*)/T_0^*$ is of the order of M_∞^2 which is smaller than ϵ^2 for water and is considerably smaller than that due to surface heating.

In the main deck and the outer deck, the unsteady term and the diffusion terms are at least one order higher than the convection terms, the leading equations in these two layers remain the same as those for the standard triple deck, i.e., they are quasisteady and uncoupled from the energy equation. The velocity components in the main deck deviate from the boundary-layer profile at $x^* = L^*$ by $\epsilon^2 u^{(2)}$ and $\epsilon^3 v^{(3)}$, respectively. The solutions are[7,13]

$$u^{(2)}(x,y,t) = A(x,t)U_B'(y) \tag{9a}$$

and

$$v^{(3)}(x,y,t) = -A_x(x,t)U_B(y) \tag{9b}$$

The solutions in the main deck represent passive responses to the disturbances at the outer edge of the inner deck with

$$A(x,t) = \beta^{-1}\bar{u}^{(2)}(x,\infty,t) \tag{10}$$

In the outer deck the perturbation velocity and the pressure are of the order ϵ^3 and obey the potential equation and the linearized Bernoulli equation. In particular, the pressure $\bar{p}^{(3)}(x,\bar{y},t)$ on $\bar{y} = 0^+$, which is equal to $p^{(3)}(x,t)$ in the main deck, is related to $\bar{v}^{(3)}(x,\bar{y}=0^+,t)$ or $v^{(3)}(x,\infty,t)$, which is $-A_x(x,t)$, by the Hilbert transform,[7,13]

$$p^{(3)}(x,t) = \frac{1}{\pi}\int_{-\infty}^{\infty} \frac{A_\xi(\xi,t)\,d\xi}{x-\xi} \tag{11}$$

Equations (8a-c), (10), and (11) are the governing equations for the four unknowns $\bar{u}^{(2)}$, $\bar{v}^{(4)}$, $\bar{T}^{(1)}$, and $p^{(3)}$. The thermal boundary conditions on $\bar{y} = 0$ are

$$\bar{T}^{(1)} = 0, \qquad \bar{x} < 0 \text{ or } \bar{x} > b \tag{12a}$$

$$\bar{T}^{(1)} = 1 + \cos\omega t \qquad \text{on a heating strip} \tag{12b}$$

and

$$\bar{T}^{(1)} = 1 \qquad \text{in between heating strips} \tag{12c}$$

where $\omega = 2\omega^* U_\infty^*/(L\epsilon^2)$. The nonslip conditions on $\bar{y} = 0$ are

$$\bar{u}^{(2)} = 0 \text{ and } \bar{v}^{(4)} = 0 \tag{13}$$

The upstream and downstream conditions are

$$\bar{u}^{(2)} \to 0, \quad \bar{T}^{(1)} \to 0, \text{ and } p^{(3)} \to 0 \text{ as } x \to -\infty \tag{14a}$$

and

$$p^{(3)} \to 0 \quad \text{as } x \to \infty \tag{14b}$$

Solutions (9a) and (9b) fulfill the matching conditions on velocity. The thermal condition is

$$\bar{T}^{(1)} \to 0 \text{ as } \bar{y} \to \infty \tag{15}$$

The initial conditions are

$$\bar{T}^{(1)} = \bar{u}^{(2)} = \bar{v}^{(4)} = p^{(3)} = 0 \tag{16}$$

at $t = 0$ which is the instant we turn on the heat. We replace Eq. (16) by the periodic condition when we look for the periodic solution induced by the periodic term in the thermal boundary condition (12b).

We note that Eq. (8c) for the temperature is uncoupled from the rest. In the next section we shall solve Eq. (8c) subjected to the boundary conditions and initial conditions on $\bar{T}^{(1)}$.

III. The Temperature Profile

Since the problem is linear, the solution for several strips can be constructed by superposition of the solution for a single strip. The latter in turn is a superposition of the canonical solution for which the wall temperature is $H(x)e^{-i\omega t}$ where H is the Heaviside function. We shall then outline how to construct the canonical solution.

We note that Eq. (8c) contains two parameters, β and Pr. They can be removed by introducing the new variables

$$\xi = \sqrt{Pr}x/\beta \text{ and } \eta = \sqrt{Pr}\bar{y} \tag{17}$$

so that the canonical solution $\theta(\xi,\eta,t,\omega)$ is independent of Pr and β. Equation (8c) becomes

$$\theta_t + \eta\theta_\xi = \theta_{\eta\eta} \tag{18}$$

The boundary conditions and the periodicity conditions are

$$\theta = e^{i\omega t} \text{ on } \eta = 0, \quad \xi > 0 \tag{19a}$$

$$\theta = 0 \quad \text{on } \xi = 0, \quad \eta > 0 \tag{19b}$$

$$\theta \to 0 \quad \text{as } \eta \to \infty \tag{19c}$$

and

$$\theta(\xi,\eta,t,\omega) = \psi(\xi,\eta,\omega)e^{i\omega t} \tag{19d}$$

Condition (19b) replaces the upstream condition (14a) on $\bar{T}^{(1)}$, which together with Eq. (12a) implied $\theta = 0$ for $\xi \le 0$ except $\xi = \eta = 0$.

When $\omega = 0$, we have a steady problem. The steady temperature profile is defined by a similarity solution,

$$\theta(\xi,\eta) = g_0(\zeta) \tag{20}$$

where the similarity variable ζ is

$$\zeta = \eta/(9\xi)^{1/3} \tag{21}$$

Equation (18) becomes $g_0'' + 3\zeta^2 g_0' = 0$. The boundary conditions are $g_0(0) = 1$ and $g_0(\infty) = 1$. The solution is

$$g_0'(\zeta) = -3e^{-\zeta^3}/\Gamma(1/3) \tag{22a}$$

and

$$g_0(\zeta)=\Gamma(\tfrac{1}{3},\zeta^3)/\Gamma(\tfrac{1}{3}) \tag{22b}$$

where $\Gamma(\frac{1}{3}, z)$ is an incomplete gamma function of z.[17] We note that $g_0(\zeta)$ decays exponentially in ζ^3.

For $\omega\neq 0$, we change the variables ξ, η to ξ, ζ and seek periodic solution $\phi(\xi, \zeta, \omega)\, e^{i\omega t}$. ϕ obeys

$$\text{D.E.}\quad \phi_{\zeta\zeta}+3\zeta^2\phi_\zeta-9\zeta\xi\phi_\xi-i\omega(9\xi)^{1/3}\phi=0 \tag{23}$$

$$\text{B.C.}\quad \phi(\xi,\zeta=0)=1 \text{ and } \phi(0,\zeta\to\infty)=0 \tag{24}$$

We assume that ϕ can be represented by a power series in ω for a sufficiently small ω. The first term is independent of ω and hence is a quasisteady solution, the same as $g_0(\zeta)$. The series solution for $\phi(\xi, \zeta, \omega)$ can be written as

$$\phi\sim g_0(\zeta)+\sum_{n=1,2,\ldots}[i\omega(9\xi)^{1/3}]^n g_n(\zeta) \tag{25}$$

for $\xi\geq 0$ and $\phi=0$ for $\xi<0$. Equations (23) and (24) become

$$g_n''+3\zeta^2 g_n'-6n\zeta g_n=g_{n-1} \tag{26}$$

$$g_n(0)=0 \text{ and } g_n(\infty)=0 \tag{27}$$

for $n=1,2,\ldots$. A particular solution, g_n^p, of Eq. (26) can be shown to be

$$g_n^p=a_n[3\zeta^2 g_{n-1}+g_{n-1}'] \tag{28}$$

where $a_n=1/(6n+a_{n-1})$, and $a_0=0$. Note that g_n^p decays exponentially in ζ^3 when g_{n-1} does. Let g_{n1} and g_{n2} denote respectively the first and second fundamental solutions of Eq. (26). Both g_{n1} and g_{n2}/ζ are represented by power series in ζ^3 which converges for all ζ. The general solution of Eq. (26) fulfilling the condition at $\zeta=0$ is

$$g_n(\zeta)=g_n^p(\zeta)-g_n^p(0)[g_{n1}(\zeta)+\lambda_n g_{n2}(\zeta)] \tag{29}$$

Both g_{n1} and g_{n2} behave as ζ^{2n} for large ζ. The boundary condition at infinity defines λ_n such that $g_{n1}+\lambda_n g_{n2}$ does not contain the ζ^{2n} term. We can show that $g_n(\zeta)$ decays exponentially in ζ^3 for $n=0,1,2,\ldots$. Details are presented in Appendix A of the preprint.[18]

In particular for $n=1$, we have $a_1=1/6$, $g_1^p=[3\zeta^2 g_0+g_0']/6$, $g_1^p(0)=-1/[2\Gamma(\frac{1}{3})]$ and $\lambda_1=-1.533$. The temperature given by the real part of the first two terms of the series solution (25) is

$$\bar\theta(\xi,\eta,t,\omega)=[g_0(\zeta)\cos\omega t-\omega(9\xi)^{1/3}g_1(\zeta)\sin\omega t]H(\xi) \tag{30}$$

The temperature profile induced by J heating strips with wall temperature specified by Eqs. (12a-c) is

$$\begin{aligned}\bar T_j^{(1)}(x,\bar y,t)&=\{g_0(\zeta)H(\xi)-g_0(\zeta_J)H(\xi_J')\}\\&+\cos\omega t\sum_{j=1}^{J}\{g_0(\zeta_j)H(\xi_j)-g_0(\zeta_j')H(\xi_j')\}\\&-\omega\sin\omega t\sum_{j=1}^{J}\{(9\xi_j)^{1/3}g_1(\zeta_j)H(\xi_j)-(9\xi_j')^{1/3}g_1(\zeta_j')H(\xi_j')\}\end{aligned} \tag{31}$$

where $\xi_j=(x-x_j)\sqrt{Pr}/\beta$, $\xi_j'=\xi_j+\ell_j\sqrt{Pr}/\beta$, $\zeta_j=\eta/(9\xi_j)^{1/3}$ and $\zeta_j'=\eta/(9\xi_j')^{1/3}$. For solution (31), all the heating strips are in phase and the abscissas of the leading and trailing edge of the jth strip are x_j and $x_j+\ell_j$ with $x_1=0$ and $x_J+\ell_J=b$. Solution (31) is composed of the steady and the first two order unsteady solutions.

Since the maximum of $|g_1(\zeta)|$ is only 5% of that of $|g_0(\zeta)|$, it is expected that the correction term to the unsteady effect, i.e., the term containing $\omega\sin\omega t$ in Eq. (30) and that in Eq. (31) are numerically small for $\omega(9x\sqrt{Pr}/\beta)^{1/3}\leq 1$. This fact is also demonstrated in the numerical results for the temperature profile shown in Figs. 2 and 3 of Ref. 18.

In the next section, the velocity and pressure disturbances induced by the viscosity temperature dependence, i.e., the forcing term $\Lambda\beta\bar T_y^{(1)}$ in Eq. (8b), are constructed. The temperature profile employed contains only the steady term and the quasisteady term, i.e., the first two terms in Eq. (31). The last term which is proportional to $\omega\sin\omega t$ will be neglected on the assumption that the scaled frequency ω is small.

IV. Pressure and Velocity Disturbances

The disturbance velocity components $\bar u^{(2)}$ and $\bar v^{(4)}$ in the inner deck and the disturbance pressure $p^{(3)}$ across the inner

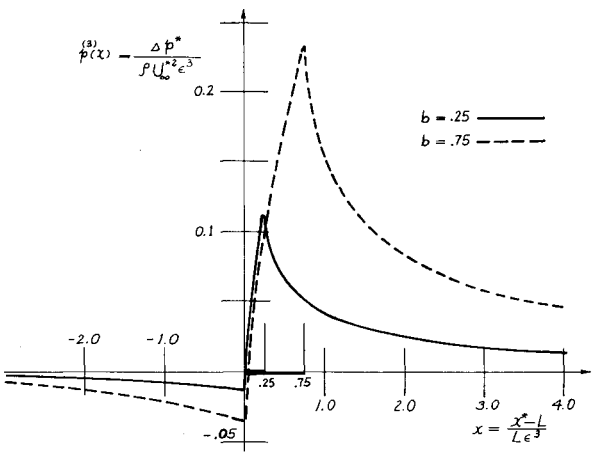

Fig. 2 Pressure disturbances induced by steady surface heating.

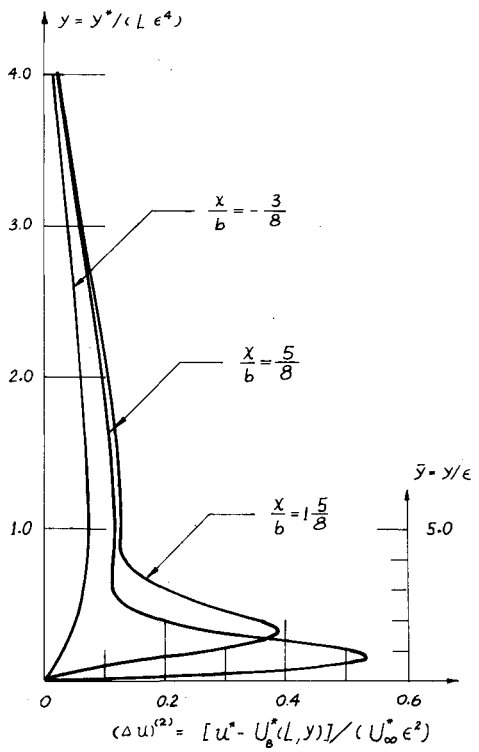

Fig. 3 Velocity disturbances in the lower and main decks for $\epsilon=0.2$.

and the main deck are governed by a system of the partial differential equations (8a) and (8b) and the integral equation (11). The last terms $\Lambda\beta\bar{T}_{\bar{y}}^{(1)}$ in Eq. (8b) is the forcing term in which $\bar{T}^{(1)}$ is determined in the preceding section as superpositions of a canonical similarity solution. We shall represent the disturbance velocity as superpositions or linear combinations of two canonical solutions of ordinary differential equations in the similarity variable $\bar{y}/x^{1/3}$. The coefficients of the linear combinations are then determined by a system of linear algebraic equations which are obtained by equating the pressure required to balance the momentum equation (8b) with that defined by Eq. (11).

Let $\bar{\psi}(x,\bar{y})e^{-i\omega t}$ and $p_0(x)e^{-i\omega t}$ represent the quasisteady stream function of $\bar{u}^{(2)}$ and $\bar{v}^{(4)}$ and $p^{(3)}(x,t)$, respectively. For small ω, Eqs. (8a) and (8b) become

$$\mathcal{L}\bar{\psi}=\left(\beta\bar{y}\frac{\partial^2}{\partial x\partial\bar{y}}-\beta\frac{\partial}{\partial x}-\frac{\partial^3}{\partial\bar{y}^3}\right)\bar{\psi}=-p_0'(x)+\beta\Lambda\bar{T}_{\bar{y}} \tag{32}$$

We shall decompose the stream function $\bar{\psi}$ into two parts

$$\bar{\psi}=\beta\Lambda\Psi(x,\bar{y})+\hat{\psi}(x,\bar{y}) \tag{33}$$

The factor $\beta\Lambda$ is introduced so that the particular solution will be independent of Λ and β. Ψ fulfills

$$\mathcal{L}\Psi=\bar{T}_{\bar{y}}-P'(x) \tag{34}$$

and the nonslip conditions,

$$\Psi=\Psi_{\bar{y}}=0 \tag{35a}$$

on $\bar{y}=0$ and the extra condition,

$$\Psi_{\bar{y}}(x,\bar{y}\to\infty)=0 \tag{35b}$$

Ψ is a particular solution induced by the viscosity-temperature variation term with the appropriate pressure $P(x)$ in Eq. (34) such that Eq. (35b) holds. The solution can be constructed by superpositions of a canonical solution which is induced by a single semi-infinite heating strip, $x>0$. It is a similarity solution which is defined in the Appendix and the corresponding pressure $P(x)$ in Eq. (34) is shown to be proportional to $x^{2/3}H(x)$.

For example, for a single heating strip $0<x<b$, the pressure for the particular solution is

$$P(x)=\lambda_0 3(3Pr\beta)^{1/3}[x^{2/3}H(x)-(x-b)^{2/3}H(x-b)] \tag{36}$$

where the constant λ_0 is defined in the Appendix.

Because of Eq. (35b) the pressure defined by the Hilbert transform Eq. (11) is zero. To balance the discrepancy between $\Lambda\beta P(x)$ and zero pressure from Eq. (11), we need the second part $\hat{\psi}$ in Eq. (33). It fulfills Eq. (32) without the forcing term, i.e.,

$$\mathcal{L}\hat{\psi}=-\hat{p}'(x) \tag{37}$$

and the nonslip conditions

$$\hat{\psi}(x,0)=\hat{\psi}_{\bar{y}}(x,0)=0 \tag{38}$$

The pressure $\hat{p}(x)$ in Eq. (37) should be such that its sum with $\Lambda\beta P(x)$ for the particular solution Ψ in Eq. (34) should be equal to the pressure $p_0(x)$ defined by Eq. (11), i.e.,

$$\hat{p}(x)+\Lambda\beta P(x)=p_0(x) \tag{39}$$

with

$$p_0(x)=\frac{1}{\pi}\int_{-\infty}^{\infty}\frac{A_0'(\xi)\,d\xi}{x-\xi} \tag{40a}$$

and

$$A_0(x)=\beta^{-1}\hat{\psi}_{\bar{y}}(x,\bar{y}\to\infty) \tag{40b}$$

It is evident that $\beta\Lambda\Psi+\hat{\psi}$ and p_0 are the quasisteady solution of Eqs. (8a), (8b) and (11) fulfilling the nonslip condition on $\bar{y}=0$.

To construct numerical solutions for $\hat{\psi}$, we approximate $\hat{\psi}_{\bar{y}}(x,\infty)$ by step functions, i.e.,

$$\hat{\psi}_{\bar{y}}(x,\infty)=c_j \text{ for } (j-1)\Delta<x+M\Delta<j\Delta \tag{41a}$$

$j=1,2,\ldots,M+N$ and

$$\hat{\psi}_{\bar{y}}(x,\infty)=0 \text{ for } x<-M\Delta \text{ or } x>N\Delta \tag{41b}$$

where Δ is the grid size, c_j's are unknown constants, and M and N are two sufficiently large positive integers such that the upstream and downstream conditions (14a, b) can be approximated by Eq. (41b). The solution $\hat{\psi}$ is represented by a linear combination of the canonical solution $\chi(x,\bar{y})$ as follows

$$\hat{\psi}(x,\bar{y})=\sum_{j=1,2}^{M+N}c_j[\chi(x_{j-1},\bar{y})-\chi(x_j,\bar{y})] \tag{42}$$

where $x_j=x-M\Delta+j\Delta$. $\chi(x,\bar{y})$ is the canonical solution and is a similarity solution of Eq. (37) subjected to the nonslip condition (38) and the imposed condition that the far-field velocity for the inner deck is a Heaviside function of x, i.e.,

$$\chi_{\bar{y}}(x,\infty)=H(x) \tag{43}$$

The corresponding pressure field in Eq. (37) should be $\alpha\beta(x/\beta)^{1/3}H(x)$. The canonical solution χ and the constant α are defined in the Appendix.

For $\hat{\psi}_{\bar{y}}(x,\infty)$ defined by Eqs. (41a) and (41b), the pressure field defined by the Hilbert transform Eq. (40a) is

$$p_0(x)=\frac{1}{\beta\pi}\sum_{j=1}^{N+M}{}'c_j\left[\frac{1}{x_{j-1}}-\frac{1}{x_j}\right] \tag{44}$$

The prime over the summation sign indicates that the term $1/x_{j-1}$ or $1/x_j$ will be omitted whenever the denominator vanishes.

The pressure field required in Eq. (37) for $\hat{\psi}$ given by Eq. (42) is

$$\hat{p}=\alpha\beta^{2/3}\sum_{j=1,2}^{M+N}c_j[(x_{j-1})^{1/3}H(x_{j-1})=(x_j)^{1/3}H(x_j)] \tag{45}$$

For a single heating strip the pressure $P(x)$ due to the particular solution Ψ is defined by Eq. (36). With $\hat{p}(x)$ and $p_0(x)$ related to the constants c_j by Eqs. (45) and (44), respectively, Eq. (39) becomes the equation to define c_j. By imposing Eq. (39) at mid-grid points $x=-M\Delta+(j-\frac{1}{2})\Delta$ for $j=1,\ldots,M+N$, Eq. (39) becomes $M+N$ linear algebraic equations for c_j. Thus the c_j's for a single heating strip and hence the corresponding quasisteady solution are determined. By the method of superposition, we can construct a solution for several heating strips with surface temperature composed of steady and periodic terms with different phases and frequencies.

V. Numerical Results and Boundary-Layer Control

Numerical results are obtained for water with $T_0^*=10°C$, $Pr=9.5$ and $\Lambda=(T^*/\nu^*)(d\nu^*/dT^*)=-7.2$. The regular boundary-layer profile without surface heating is assumed to be the Blasius profile $U_\infty U_B'(y)$ with $\beta=U_B'(0)=0.332$.

Figure 2 shows the pressure variation induced by a single heating strip with scaled strip width equal to 0.25 and 0.75,

respectively. It represents the steady or quasisteady solution. As x increases, the pressure signature decreases slightly below zero ahead of the leading edge of the strip, $x<0$, increases drastically to the maximum value at the trailing edge, $x=b$, and decreases drastically at first and then gradually to zero for $x>b$. The pressure signature bears very strong resemblance to that induced by a single porous suction strip.[14] Thus the numerical results demonstrate the equivalence between surface heating and suction for water proposed by Liepmann et al.[2,3]

To show that steady surface heating does induce favorable changes in velocity profile, we construct the composite solution of the velocity profile in the inner and main deck from Eqs. (7b), (9a), and (10). It is

$$u(x,y,\epsilon)=U_B(y)+\epsilon^2[\bar{u}^{(2)}(x,\bar{y})-\bar{u}^2(x,\infty)+u^{(2)}(x,y)]+\mathcal{O}(\epsilon^3)=U_B(y)+\epsilon^2[\bar{u}^{(2)}(x,\bar{y})-\bar{u}^{(2)}(x,\infty)+\bar{u}^{(2)}(x,\infty)U_B'(y)/\beta]+\mathcal{O}(\epsilon^3) \quad (46)$$

The terms inside the square bracket, denoted by $(\Delta u)^{(2)}$ equal $u^{(2)}(x,y)$ and $\bar{u}^{(2)}(x,\bar{y})$ in the main deck and the lower deck, respectively. $(\Delta u)^{(2)}$ represents the velocity deviation scaled by $\epsilon^2 U_\infty$. Figure 3 shows the profiles of $(\Delta u)^{(2)}$ at stations ahead, inside, and behind the heating strip, respectively, for $b=0.75$, $\epsilon=0.2$, i.e., $\bar{y}=5y$. At all three stations $(\Delta u)^{(2)}$ is nonnegative, decreasing in the main deck, and vanishes exponentially at the outer edge of the main deck or of the boundary layer. In the lower deck, the profile of $(\Delta u)^{(2)}$ of the first station differs remarkably from those of the other two. At the first station, $x<0$, the thermal forcing term in Eq. (32) and hence the particular solution ψ vanishes. $\Delta u^{(2)}$ is then equal to $\hat{\psi}_{\bar{y}}$ induced by the pressure gradient $p_x^{(3)}$ in Eq. (32) which is induced by the pressure variation $\bar{p}^{(3)}$ in the outer deck through Eq. (11). Since $p_x^{(3)}$ is favorable in $x<0$ (see Fig. 2), $(\Delta u)^{(2)}$ increases in the lower deck and reaches its maximum value at the overlapping region of the lower and the main deck. For $x>0$, the thermal forcing term in Eq. (32) dominates the pressure gradient term, hence the unfavorable p_x in $0<x<b$ (see Fig. 2) does not change the character of the profile of $(\Delta u)^{(2)}$. With $(\Delta u)^{(2)}$ equal to $\hat{\psi}_y+\beta\Lambda\Psi_{\bar{y}}$, $(\Delta u)^{(2)}$ is dominated by the second term which reaches its maximum inside the lower deck and spreads as x increases. The profiles of $(\Delta u)^{(2)}$ for $x>b$ behave in the same manner. Thus the numerical results confirm the statement in Sec. I that surface heating induces additional momentum near the wall and makes the velocity profile fuller and less prone to separation.

To study the effect on stability, we compute the change of the dimensionless displacement thickness. From Eq. (46) we obtain

$$\frac{\delta^*(x)-\delta_B^*(L)}{\epsilon^4 L}=-\int_0^\infty[u(x,y,\epsilon)-U_B(y)]\,dy=-\epsilon^2\bar{u}^{(2)}(x,\infty)/\beta+\mathcal{O}(\epsilon^3) \quad (47)$$

For the Blasius profile we have $\delta_B^*(L)/(\epsilon^4 L)=1.7208$. Figure 4 shows the change in displacement thickness induced by a single heating strip with $b=0.25$ and 0.75, respectively. The numerical value of $\bar{u}^{(2)}(x,\infty)$ is positive for all x. This result is of course consistent with Fig. 3 and the statement that surface heating adds momentum to the lower deck. Equation (48) and Fig. 4 show that surface heating reduces the displacement thickness, makes the velocity profile fuller, and enhances stability.

The preceding results are applicable to steady surface heating. When surface heating is generated by an alternating current of frequency ω^*, the surface temperature, defined by Eq. (2), is composed of a steady term and a periodic term. The disturbed flowfield in the triple deck is composed of the steady solution and the quasisteady solution due to the periodic term. Figure 5 shows the induced pressure disturbance due to two heating strips placed in the intervals $0\le x\le 0.25$ and $0.5\le x\le 0.75$ at the instants $\omega t=0$, $\pi/2$, and π, respectively. The surface temperature is given by Eqs. (12a-c). The heating strips are in phase, and the scaled temperature oscillates between two (at $\omega t=0$) and zero (at $\omega t=\pi$). The temporal fluctuation of the disturbance pressure is demonstrated in Fig. 5.

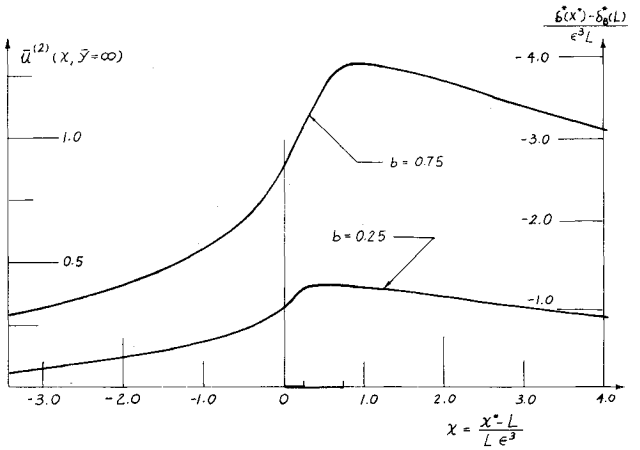

Fig. 4 Displacement thickness variations.

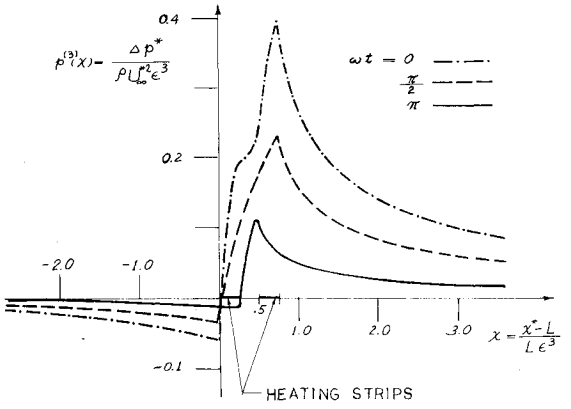

Fig. 5 Temporal variations of the pressure disturbances.

In general we can construct the linear triple-deck solutions for several heating strips with assigned phase differences by superpositions of solutions for a single heating strip. These numerical results shall then serve as the input data to study the interaction of the actively controlled disturbances due to surface heating with the T-S waves.

VI. Concluding Remarks

Linear triple-deck analysis has been carried out for incompressible flow over a flat plate with surface heating of small temperature variation of the order $\epsilon=(Re)^{-1/8}$. The heating strips are narrow so that their total width is of the order of $\epsilon^3 L$ and the strips are embedded in the triple deck at $x^*=L$. Re is the Reynolds number with length L. The scalings are consistent with the experiments of Liepmann et al. The analysis and the numerical results confirm the results of Liepmann et al. that localized low surface heating is quite effective for boundary-layer control for water. We show that the surface heating creates the following conditions.

1) A normal velocity disturbance and a pressure disturbance of the order ϵ^3 or $\epsilon^{-1}/\sqrt{Re}$ in the main deck, i.e., the majority of the boundary layer. Both disturbances are one

order larger than those quantities in a regular boundary layer.

2) The thermal layer is embedded in the lower deck and solved. Its thickness is that of the lower deck, i.e., $\epsilon^5 L$ for steady or unsteady heating with angular frequency ω^* of the order of $(U_\infty/L)\epsilon^2$. When the frequency is much larger than that, the unsteady thermal layer becomes much thinner than the inner deck and becomes ineffective. When the frequency is much smaller than that, the thermal layer is dominated by the quasisteady solution which is equal to the steady solution with wall temperature depending on t as a parameter.

3) Due to the dependence of viscosity on temperature for water, the thermal effect adds momentum to the inner and main deck. The velocity disturbance reaches its maximum inside the inner deck near the maximum of the particular solution $\beta\Lambda\Psi_{\bar{y}}$ or in the overlapping region of the inner and the main deck when Ψ is zero ahead of the heating strips and then decreases to zero exponentially near the outer edge of the main deck. Thus steady localized low surface heating induces a favorable profile which is fuller with thinner displacement thickness and hence delays separation and the onset of instability.

4) Surface heating generated by alternating current can actively control the waveform and the frequency of the induced disturbances in the triple deck. Our analysis provides the solutions of the velocity and pressure disturbances when the scaled frequency is small, $\omega \ll 1$. The solutions shall then serve as the input data to study whether the induced disturbances will enhance or cancel the T-S waves. If the scaled frequency is finite, $\omega = \mathcal{O}(1)$, the full unsteady analyses for the energy equation and then the momentum equation in the inner deck have to be carried out.

For air the dependence of viscosity on temperature, i.e., $d\ell n\mu/d\ell nT$ is much weaker than that for water and is of opposite sign. A steady surface heating for air would produce an opposite effect, i.e., the velocity will be less favorable. Furthermore, a finite change in the steady and the periodic wall temperature is needed for air to induce the same order of magnitude of disturbances in velocity and pressure as that for water. Consequently a nonlinear triple-deck analysis has to be carried out to study the effect of surface heating on boundary-layer control for air.

Appendix: Particular and Canonical Solutions for the Velocity Profile

From Sec. III we see that the temperature profile is a superposition of terms of the type $(9\xi)^{2n/3}\, g_n(\zeta)$. The inhomogeneous term due to the viscosity temperature variation in the momentum equation (34) is composed of terms of the type $(9\xi)^{(2n-1)/3}\, g_n'(\zeta)$. We shall construct the particular solution Ψ for each n with the appropriate pressure $P(x)$ such that $\Psi_{\bar{y}}$ vanishes for large $\bar{y}$. With

$$\Psi_n = (9\xi)^{2(n+1)/3} F_n(\zeta) e^{i\omega t}$$

and

$$P_n = \lambda_n \beta (9\xi)^{2(n+1)/3} e^{i\omega t} \tag{A1}$$

Eqs. (34) and (35) become

$$PrF_n''' + 3\zeta^2 F_n'' - 6(n+1)[\zeta F_n' - F_n] = 6(n+1)\lambda_n - g_n'(\zeta) \tag{A2}$$

$$F_n(0) = F_n'(0) = 0 \text{ and } F_n'(\infty) \to 0 \tag{A3}$$

For $n=0$, two homogeneous solutions are ζ and ζ^2. The third one is given by an improper integral from ζ to ∞. We can then proceed to construct the particular solution, find its asymptotic behavior, and then determine the three coefficients and the parameter λ_0 to fulfill Eq. (A3). This is a tedious process. Furthermore, in the construction of the velocity profiles in Fig. 3, we have to compute $F_0(\zeta)$ for each point (x,y). It will be much faster to evaluate $F_0(\zeta)$ by its power series and asymptotic formulas than by the integral representation. Therefore, we proceed to determine the power series and its asymptotic behavior of F_n directly, using the standard method for a two-point boundary value problem. We represent the solution F_n by three parts,

$$F_n = KH(\zeta) + 6(n+1)\lambda_n P_1(\zeta) + P_2(\zeta)$$

where $K = F_n''(0)/2$. $H(\zeta)$ is the homogeneous solution fulfilling the boundary conditions $H(0) = H'(0) = 0$ and $H''(0) = 1$. P_1 and P_2 are the particular solutions fulfilling the boundary conditions $P_i(0) = P_i'(0) = P_i''(0) = 0$ and the inhomogeneous terms are 1 and $-g_n$ for $i = 1, 2$, respectively. Power series representations of the H and P_i shall then be obtained. For large ζ, F_n and also H and P_i behave in general as

$$F_n = k_2 Q_n(\zeta) + k_1\zeta + k_0 + \mathcal{O}[\exp(-\zeta^3)]$$

Here Q_n is a polynomial of degree $2n+2$ descending in powers of ζ^3 and is a homogeneous solution. However, when $2n+1$ is divisible by 3, the last term ζ shall be replaced by $\zeta\ell n\zeta$ plus an asymptotic series beginning with ζ^{-2}. By patching the asymptotic series with the power series, say, near $\zeta = 3$, the coefficients k_m^i (for $m = 0,1,2$ with $i = 0$ for H, $i = 1,2$ for P_i) can be determined. Finally we find the unknown K and λ_n from the equations

$$Kk_n^0 + 6(n+1)\lambda_n k_m^1 + k_m^2 = 0 \text{ for } m = 1,2$$

They insure that $F_n'(\infty) \to 0$, i.e., $k_2 = k_1 = 0$.

For $n=0$, we have

$$Q_0 = H = \zeta^2, \quad p_1 = \sum_{j=1}^{\infty} q_j \zeta^{3j}$$

and

$$P_2 = [3/\Gamma(\tfrac{1}{3})] \sum_{j=1}^{\infty} d_j \zeta^{3j}$$

where

$$d_j = [(-1)^j/(j!) - 3(3j-4)(3j-5)d_{j-1}] \div [3j(3j-1)(3j-2)Pr]$$

and

$$q_j = [-(3j-4)(3j-5)q_{j-1}]/[j(3j-1)(3j-2)Pr]$$

for $j = 2,3,\ldots$, with $d_1 = q_1 = 1/(6\,Pr)$. For $Pr = 9.5$, $\beta = 0.332$ we have $F''(0) = -0.0621$, and $k_0 = \lambda_0 = -0.0245$. Thus the determination of the particular solution for Eqs. (34) and (35) is completed.

We shall now construct the canonical stream function χ of Eqs. (37) and (38) with the appropriate pressure gradient $\hat{p}'(x)$ such that Eq. (43) is fulfilled. The stream function χ can be represented by the similarity solution $(x/\beta)^{1/3} f(\hat{\zeta})$ where $\hat{\zeta} = y(x/\beta)^{-1/3} = \zeta(9\,Pr)^{1/3}$. We use this similarity variable $\hat{\zeta}$ because the solution shall then be independent of Pr and can be identified with the boundary-layer solution in the presence of a large shear flow.[19] The appropriate pressure is $\hat{p} = \alpha\beta(x/\beta)^{1/3}$. Equations (37), (38), and (43) become

$$3f''' + \hat{\zeta}^2 f'' - (\hat{\zeta}f' - f) = \alpha \tag{A4}$$

where $f(0) = f'(0) = 0$ and $f(\infty) \to \hat{\zeta} + \alpha$, respectively. The solution is given in Ref. 19 with $f''(0) = 0.7866$ and $\alpha = -0.8695$.

Acknowledgment

The research of Lu Ting was partially supported by NASA Langley Research Center Grant NAG-1-134.

References

[1]Schlichting, H., *Boundary Layer Theory*, 7th ed., McGraw-Hill Book Co., New York, 1979, pp. 378-402.

[2]Liepmann, H. W., Brown, G. L., and Nosenchuck, D. M., "Control of Laminar-Instability Waves Using a New Technique," *Journal of Fluid Mechanics*, Vol. 118, May 1982, pp. 187-200.

[3]Liepmann, H. W. and Nosenchuck, D. M., "Active Control of Laminar-Turbulent Transition," *Journal of Fluid Mechanics*, Vol. 118, May 1982, pp. 201-204.

[4]Nosenchuck, D. M., "Active and Passive Control of Boundary Layer Transition," Ph.D. Thesis, California Institute of Technology, Pasadena, Calif., 1982.

[5]Messiter, A. F., "Boundary Layer near the Trailing Edge of a Flat Plate," *SIAM Journal on Applied Mathematics*, Vol. 18, Jan. 1970, pp. 241-257.

[6]Stewartson, K., "On the Flow Near the Trailing Edge of a Flat Plate, II," *Mathematika*, Vol. 16, June 1969, pp. 106-121.

[7]Stewartson, K., "Multistructured Boundary Layers on Flat Plates and Related Bodies," *Advanced Applied Mechanics*, Vol. 14, Academic Press, New York, 1974, pp. 145-239.

[8]Brown, S. N. and Daniels, P. G., "On the Viscous Flow about the Trailing Edge of a Rapidly Oscillating Plate," *Journal of Fluid Mechanics*, Vol. 67, Feb. 1975, pp. 743-762.

[9]Chow, R. and Melnik, R. E., "Numerical Solutions of the Triple-Deck Equations for Laminar Trailing Edge Stall," *Proceedings of the 5th International Conference on Numerical Methods in Fluid Dynamics, Lecture Notes in Physics*, Vol. 59, Springer-Verlag, 1976, pp. 135-144.

[10]Messiter, A. F. and Linan, A., "The Vertical Plate in Laminar Free Convection: Effects of Leading and Trailing Edges and Discontinuous Temperature," *Zeitschrift fuer Angewandte Mathematik und Physik*, Vol. 27, Sept. 1976, pp. 633-651.

[11]Rizzetta, D. P., "Asymptotic Solutions of the Energy Equation for Viscous Supersonic Flow Past Corners," *Physics of Fluids*, Vol. 22, Feb. 1979, pp. 218-223.

[12]Smith, F. T., "On the Non-parallel Flow Stability of the Blasius Boundary Layer," *Proceedings of the Royal Society of London*, Series A, Vol. 366, May 1979, pp. 91-109.

[13]Smith, F. T., "On the High Reynolds Number Theory of Laminar Flows," *IMA Journal of Applied Mathematics*, Vol. 28, May 1982, pp. 207-281.

[14]Nayfeh, A. H., Reed, H. L., and Ragab, S. A., "Flow Over Plates with Suction Through Porous Strips," *AIAA Journal*, Vol. 20, May 1982, pp. 587-588.

[15]Cheng, H. K. and Smith, F. T., "The Influence of Airfoil Thickness and Reynolds Number on Separation," *Zeitschrift fur Angewandte Mathematik und Physik*, Vol. 33, March 1982, pp. 151-180.

[16]Meyer, R. E., "A View of the Triple Deck," *SIAM Journal on Applied Mathematics*, Vol. 43, Aug. 1983, pp. 639-663.

[17]Abramowitz, A. and Stegun, I. R., *Handbook of Mathematical Functions*, National Bureau of Standards Applied Mathematics Series, No. 55, 1973, pp. 253-263.

[18]Maestrello, L. and Ting, L., "Anlaysis of Active Control by Surface Heating," AIAA Paper 84-0173, Jan. 1984.

[19]Ting, L., "Boundary Layer over a Flat Plate in Presence of Shear Flow," *Physics of Fluids*, Vol. 3, Jan. 1960, pp. 78-81.